

ECCM



26-30 JUNE

2022

LAUSANNE
SWITZERLAND



Proceedings of the 20th European Conference on Composite Materials

COMPOSITES MEET SUSTAINABILITY

Vol 1 – Materials

Editors : Anastasios P. Vassilopoulos, Véronique Michaud

Organized by :

Under the patronage of :

CCLAB
Composite
Construction
Laboratory

LPAC
Laboratory for Processing
of Advanced Composites

ESCM
EUROPEAN SOCIETY
FOR COMPOSITE MATERIALS

**Proceedings of the 20th
European Conference on Composite Materials
ECCM20
26-30 June 2022,
EPFL Lausanne Switzerland**

Edited By :

Prof. Anastasios P. Vassilopoulos, CCLab/EPFL

Prof. Véronique Michaud, LPAC/EPFL

Organized by:

Composite Construction Laboratory (CCLab)

Laboratory for Processing of Advanced Composites (LPAC)

Ecole Polytechnique Fédérale de Lausanne (EPFL)

ISBN: 978-2-9701614-0-0

DOI: http://dx.doi.org/10.5075/epfl-298799_978-2-9701614-0-0

Published by :

Composite Construction Laboratory (CCLab)
Ecole Polytechnique Fédérale de Lausanne (EPFL)
BP 2225 (Bâtiment BP), Station 16
1015, Lausanne, Switzerland

<https://cclab.epfl.ch>

Laboratory for Processing of Advanced Composites (LPAC)
Ecole Polytechnique Fédérale de Lausanne (EPFL)
MXG 139 (Bâtiment MXG), Station 12
1015, Lausanne, Switzerland

<https://lpac.epfl.ch>

Cover:

Swiss Tech Convention Center
© Edouard Venceslau - CompuWeb SA

Cover Design:

Composite Construction Laboratory (CCLab)
Ecole Polytechnique Fédérale de Lausanne (EPFL)
Lausanne, Switzerland

©2022 ECCM20/The publishers

The Proceedings are published under the CC BY-NC 4.0 license in electronic format only, by the Publishers.

The CC BY-NC 4.0 license permits non-commercial reuse, transformation, distribution, and reproduction in any medium, provided the original work is properly cited. For commercial reuse, please contact the authors. For further details please read the full legal code at <http://creativecommons.org/licenses/by-nc/4.0/legalcode>

The Authors retain every other right, including the right to publish or republish the article, in all forms and media, to reuse all or part of the article in future works of their own, such as lectures, press releases, reviews, and books for both commercial and non-commercial purposes.

Disclaimer:

The ECCM20 organizing committee and the Editors of these proceedings assume no responsibility or liability for the content, statements and opinions expressed by the authors in their corresponding publication.

Editorial

This collection gathers all the articles that were submitted and presented at the 20th European Conference on Composite Materials (ECCM20) which took place in Lausanne, Switzerland, June 26-30, 2022.

ECCM20 is the 20th edition of a conference series having its roots back in time, organized each two years by members of the European Society of Composite Materials (ESCM).

The ECCM20 event was organized by the Composite Construction laboratory (CCLab) and the Laboratory for Processing of Advanced Composites (LPAC) of the Ecole Polytechnique Fédérale de Lausanne (EPFL).

The Conference Theme this year was “Composites meet Sustainability”. As a result, even if all topics related to composite processing, properties and applications have been covered, sustainability aspects were highlighted with specific lectures, roundtables and sessions on a range of topics, from bio-based composites to energy efficiency in materials production and use phases, as well as end-of-life scenarios and recycling.

More than 1000 participants shared their recent research results and participated to fruitful discussions during the five conference days, while they contributed more than 850 papers which form the six volumes of the conference proceedings. Each volume gathers contributions on specific topics:

Vol 1 – Materials

Vol 2 – Manufacturing

Vol 3 – Characterization

Vol 4 – Modeling and Prediction

Vol 5 – Applications and Structures

Vol 6 – Life Cycle Assessment

We enjoyed the event; we had the chance to meet each other in person again, shake hands, hold friendly talks, and maintain our long-lasting collaborations. We appreciated the high level of the research presented at the conference and the quality of the submissions that are now collected in these six volumes. We hope that everyone interested in the status of the European Composites’ research in 2022 will be fascinated by this publication.

The Conference Chairs

Anastasios P. Vassilopoulos, Véronique Michaud

Hosting Organizations

Composite Construction Laboratory (CCLab)
Laboratory for Processing of Advanced Composites (LPAC)
Ecole Polytechnique Fédérale de Lausanne (EPFL)

Venue

Swiss Tech Convention Center (<https://www.stcc.ch>)

Conference Chairs

Chair : Prof. Anastasios P. Vassilopoulos, EPFL, Switzerland
Co-Chair: Prof Véronique Michaud, EPFL, Switzerland

International Scientific Committee

Prof. Malin Åkermo SE	Prof. Theodoros Loutas GR
Dr. Emmanuel Baranger FR	Prof. Veronique Michaud CH
Prof. Christophe Binetruy FR	Prof. Alessandro Pegoretti IT
Prof. Pedro Camanho PT	Prof. Joao Ramoa Correia PT
Prof. Konstantinos Dassios GR	Prof. Jose Sena-Cruz PT
Prof. Brian Falzon UK	Prof. Antonio T. Marques PT
Prof. Kristofer Gamstedt SE	Prof. Thanasis Triantafillou GR
Prof. Sotiris Grammatikos NO	Prof. Albert Turon ES
Prof. Christian Hochard FR	Prof. Anastasios P. Vassilopoulos CH
Prof. Marcin Kozlowski PL	Prof. Martin Fagerström SE
Prof. Stepan Lomov BE	Dr. Alexandros Antoniou DE
Dr. David May DE	Prof. Lars Berglund SE
Prof. Stephen Ogin UK	Prof. Michal Budzik DK
Prof. Gerald Pinter AT	Prof. Lucas Da Silva PT
Prof. Silvestre Pinho UK	Dr. Andreas Endruweit UK
Prof. Yentl Swolfs BE	Prof. Mariaenrica Frigione IT
Dr. Julie Teuwen NL	Dr. Larissa Gorbatikh BE
Dr. Panayota Tsotra CH	Dr. Martin Hirsekorn FR
Prof. Wim van Paepegem BE	Prof. Vassilis Kostopoulos GR
Prof. Dimitrios Zarouchas NL	Prof. Jacques Lamon FR
Dr. Andrey Anishevich LV	Prof. Staffan Lundstrom SE
Prof. Christian Berggreen DK	Prof. Peter Mitschang DE
Dr. Nicolas Boyard FR	Dr. Soraia Pimenta UK
Prof. Valter Carvelli IT	Prof. Paul Robinson UK
Prof. Klaus Drechsler DE	Dr. Olesja Starkova LT
Prof. Bodo Fiedler DE	Prof. Sofia Teixeira de Freitas NL
Dr. Nathalie Godin FR	Dr. Stavros Tsantzalis GR
Prof. Roland Hinterholz AT	Prof. Danny van Hemelrijck BE
Prof. Ian Kinloch UK	Prof. Michele Zappalorto IT
Dr. Thomas Kruse DE	Dr. Miroslav Cerny CZ

Local Organizing Committee

Prof. Anastasios P. Vassilopoulos, EPFL
Prof. Véronique Michaud, EPFL

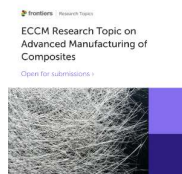
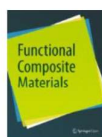
Angélique Crettenand and Mirjam Kiener, Lausanne Tourisme

And all those who helped, colleagues who reviewed abstracts and chaired sessions, and CCLab and LPAC students and collaborators who worked hard to make this conference a success.

Sponsors



A E L E R



Supporting partners



Contents

Contribution to the determination of thermal and chemical residual stresses in fiber reinforced composites using the incremental hole drilling method: numerical and experimental approach	1
A novel bio-inspired microstructure for progressive compressive failure in multidirectional composite laminates	7
Fluorescent marking of fibre reinforced plastic for component and material identification in the context of material flow canalization	14
Electrofusion welding of thermoplastic composite pipes	22
Mechanical characterisation of a long discontinuous fibre reinforced composite to evaluate the recycling potential of carbon fibre in structures	29
The mass production of MWCNTS/epoxy scaffolds using lateral belt-driven multi-nozzle electrospinning setup to enhance physical and mechanical properties of CFRP	37
Thermo-mechanical modelling of UD composites to investigate self-heating and thermal softening effect of polymer matrix	43
Towards the development of LDPE multi-layered packaging films with enhanced bioactivity	51
Investigation of 3D printed polymers and moulded composites in hot concentrated acid	59
The effect of resorcinol bis(diphenyl phosphate) on the flammability and flexibility of flame retarded epoxy gelcoats	67
Carbon and glass SMC hybrids in a sandwich arrangement	75
Investigating the effect of interface angle and ply thickness on mode II delamination behaviour of carbon/epoxy laminated composites	82
Ranking the influence of key uncertainties in the curing of thermoset laminates	90
Investigation of the mechanical properties of fuzzy CNT and CNT/CNC integrated glass fiber/epoxy composites with different reinforcing strategies	98
Mechanical properties of epoxy/carbon fiber composite fabricated by filament winding under monotonic and fatigue loadings	106
Thermoset polymer scaling effects in the microbond test	114
Ply orientation effects in multidirectional carbon/epoxy open-hole specimens subjected to shear loading	122
Carbon fibre foams: internal structure and mechanical properties	128
Study on the mode I fracture toughness of composite laminates based on the correlation between AE signal and crack front shape	136
The influence of production wastes incorporation on the properties of thermoplastic matrices	144
Extended failure models for global and local analyses of composite aerostructures	152
High strain rate characterization of twill woven carbon-polyamide laminate in longitudinal compression	160
Damage characterisation in open-hole composites using acoustic emission and finite element, validated by x-ray ct	167

An investigation on the mechanical properties of SPCS	175
Hybrid testing for composite substructures	183
Mechanical characterization of 3R-repairable composites and 3R bonding techniques produced by different processes and their repair efficiency	188
A study to improve the efficiency of laminated heating module for electric vehicles	195
Flexural behaviour of polyurethane foam filled high performance 3-d woven i-beam composites	203
Second life for aeronautical manufacturing materials	211
Development of flame retardant coatings for e-caprolactam-based polyamide 6 composites	217
Development of a carbon fiber reinforced sheet molding compound for high temperature applications	225
Development of electric vehicle underbody shield using carbon fiber/poly(ethylene terephthalate) and self reinforced polypropylene composites	233
Sustainable epoxy thermosets with potential applications in the aerospace sector	241
The influence of temperature and matrix chemistry on interfacial shear strength in glass fibre epoxy composites	249
Ceramic spatial structures as a new method of reinforcing ferrous alloys	257
Low velocity impact and residual tensile and compressive strength analysis of carbon fibre SMC composites	263
Influence of TEX linear density on mechanical properties of 3D woven i-beam composites	271
Effect of fiber microstructure on kinking in unidirectional fiber reinforced composites imaged in real time under axial compression	279
Effect of heat/fire on structural damage to carbon fibres in carbon fibre-reinforced composites	287
Use of carbon particles in fiber/epoxy UD laminates	294
Validation of composite aerostructures through integrated multi-scale modelling and high-fidelity sub-structure testing facilitated by design of experiments and BAYESIAN learning	302
Easy-repairing of high performance fibre reinforced composites with multiple healing cycles and integrated damage sensing	306
The effect of short carbon fibers on viscoelastic behavior of UHMWPE	314
Development of polypropylene melt-blown fine fiber interleaved single-polypropylene composites	322
Tailored out-of-oven curing of high performance FRPS utilising a double positive temperature coefficient effect	330
Remote activation of frontal polymerization for sustainable manufacturing of thermosets and composites	337
Sustainable multifunctional composites: from energy efficient manufacturing to integrated sensing and de-icing capabilities	344
Improved energy absorption of novel hybrid configurations under static indentation	348
Influence of brazier effect on GFRP thin circular cylinder - an experimental and numerical study	354

Multiscale interface behaviour and performance of GF-pc composite	362
Two-dimensional mode II delamination growth in composite laminates with in-plane isotropy . . .	371
Effect of lightweight fillers on the properties of polymer concrete	379
Non linear elastic behaviour of CFRP plies: material or geometrical feature?	387
Evaluation of the shear behavior of PETG/cf and pc/cf coupons manufactured using large-scale additive manufacturing processes	393
3D-print path generation of curvilinear fiber-reinforced polymers based on biological pattern forming	401
Synchrotron radiation 3D computed tomography study on in-situ mechanical damage progression of nanoengineered glass fiber reinforced composite laminates with integrated multifunctionality . . .	408
INSIGHT on induction welding of reactive PMMA carbon fiber composites	415
Litz wire-based multifunctional composites for managing thermal and mechanical loads within electrical systems	423
Shift factor dependence on physical aging and temperature for viscoelastic response of polymers . .	431
Characterization of novel sustainable composite materials based on ELIUM® 188 o resin reinforced with a Colombian natural fiber	439
Combined DIC-infrared thermography for high strain rate testing of composites	447
Effect of gap defects on in-situ AFP-manufactured structures	455
Polypropylene/flax fabric composite laminates: effects of plasma and thermal pre-treatments of reinforcing fibres	463
Improving the delamination bridging behaviour of z-pins through material selection	471
Study on the effect of strain rate and temperature on the mechanical behavior of polypropylene-glass fiber compound and thermoplastic olefin	479
Simultaneous spinning of recycled thermoplastics and glass fibers for hybrid yarns used in sustainable composites	486
Reprocessable vitrimer composites	493
Characterizing the tensile and compressive behavior of PETG/cf and pc/cf manufactured using large scale additive processes	501
Influence of mechanical properties of matrix on bending strength of uni-directional vinyl ester composite	509
Strain sensing of complex shaped 3D woven composites using MXENE nanoparticles	516
Comparison of the fire reaction of a carbon-epoxy composite at small scale and large tests	522
Efficient and versatile 3D woven composite manufacturing: novel approaches on the quality of composite fabrication	532
Electrical conductivity as an instrument for damage diagnostic of nanomodified glass fiber reinforced plastic	539
Out-of-oven manufacturing for natural fibre composites with integrated deformation and degradation sensing	547

Controlling electrical percolation in thermoplastic composites through informed selection of fillers	555
Macroscale magnetic alignment of multiple discontinuous ferromagnetic fibres in a polymer matrix	563
Laser-induced graphene carbon fiber reinforced composites for multifunctionality	569
Influence of fibre/matrix interface on gas permeability properties of CF/PVDF composites	577
Tribological study on wood and graphene reinforced high density polyethylene	585
Structural health monitoring (SHM) on fibre reinforced composite t-joint geometry manufactured by a novel 3R resin	593
The use of recycled materials towards sustainability: biocomposites manufactured in melt compounding	600
Fully bio-based epoxy-amine resins from circular economy: conception, multiscale structural and mechanical behaviour characterization toward low carbon-footprint composites	608
Mechanism-based assessment of cellulose-based biocomposite cottonid for sustainable construction	616
Novel cellulose based composite material for thermoplastic processing	624
Towards more efficient and environmental friendly flax-based eco-composite through direct F2 fluorination as a compatibilization treatment	632
Flax fibre sizings for fibre-reinforced thermosets - investigating the influences of different sizing agents on fibre moisture content and composite properties	640
Elaboration of hybrid bio-composites with thermoplastic matrix: material formulation and modelling of the quasi-static behaviour	648
Converting recycled glass fibre and polypropylene to feedstock (filament) for material extrusion additive manufacturing	656
Turning oil palm waste into all-cellulose fibreboards utilising refined pulp fibres	662
Soft composites from bio-based resources	668
All lignocellulose biocomposites for woody like materials	675
Dilatometric and fracture mechanism investigations on poly (lactic acid) PLA-calcium carbonate biocomposites	681
Effect of fibrillation of flax mat binder on the impact response of unidirectional flax/epoxy composites and comparison with a glass/epoxy composite	689
Morphological image analysis: a candid technique to determine density and geometric shapes of bio-based fibers and permanent damage due to interaction with water molecules	697
Cost-effective hemp staple fibre yarns for high-performance composite applications	705
Influence of wet/dry cycling on mechanical properties of hemp-reinforced biocomposites	713
Biodegradable polymer films to prevent biofilm formation for food packaging application	721
Life cycle assessment of natural fibre reinforced polymer composites	727
Development of quasi-unidirectional woven fabrics with 100% hemp rovings for composite materials applications	735

Effect of different natural fibres on mechanical and disintegration properties of compostable biobased plastics	743
High-strength rigid boards made from industrially produced bacterial cellulose	750
Manufacturing and mechanical characterisation of unidirectional fique fibres reinforced polypropylene composites	758
Behaviour and repair of flax/ELIUM biocomposites loaded in low velocity impact	766
On the flexural strength and actuation of wood branches – mechanisms useful in composite design?	773
Mechanical modelling of viscoelastic hierarchical suture joints and their optimization and auxeticity	779
Biobased glass fiber sizings for composites in medical and technical applications	788
The effect of humidity on the mechanical properties of flax-polyester biocomposites with different fibre architectures	795
Functionalized wood composites for mechanical energy harvesting and vibration sensing	801
Development of bio-based CFRP laminates for strengthening civil engineering structures	807
Bio-based vacuum infused glass fibre reinforced unsaturated polyester composites for high-performance structural applications	815
Hygrothermal ageing of a GFRP composite produced by vacuum infusion with a novel bio-based unsaturated polyester resin	823
Towards adhesives-free bio-based composites via UV-assisted interfacial cross-linking	831
Towards integrated health monitoring of bio-based composite structures: influence of acoustic emission sensor embedment on material integrity	838
The emerging era of visionary composites by plant-grown matrix and reinforcing fibres: the cellular adhesion	847
Lemongrass plant leaf and culm as potential sources of reinforcement for bio-composites	855
A novel method to quantify self-healing capabilities of fibre reinforced polymers	863
Enabling reparability and reuse of epoxy composites: epoxy vitrimers	871
Low velocity impact response and post impact assessment of healable CFRPS modified with diels-alder resin applied by melt electro-writing process	879
Evaluation of the self-healing capability of a polycaprolactone functionalized interphase for polymer composite applications	887
Highly conductive polypropylene based composites for bipolar plates for polymer electrolyte membrane fuel cells	894
Conductive smart nanocomposite materials for structural health monitoring and motion detection .	901
The effect of conductive network on positive temperature coefficient behaviour for multifunctional composites: from flexible sensing to sustainable manufacturing	909
Graphite filled thermoplastics for thermally conductive pipes	917
Recycling of graphitic bipolar plates for vanadium redox batteries	925

Damage sensing based on electrically conductive nanoparticles in sandwich-structured composites	933
A novel lightning strike protection system comprising an all-polymeric conductive resin	939
Low temperature growth of carbon nanotubes on fibers using copper as catalyst	945
Effect of nanoarchitecture on EMI shielding properties of nanocomposites at high content of graphite nanoplatelets	953
Rapid and facile preparation of multifunctional BUCKYPAPER nanocomposite films	961
Investigation of the thermal and mechanical properties of composite materials with amine-functionalized reduced graphene oxide inclusions	967
The application of coated carbon nanotubes in lightweight metal matrix composites	975
Nanoparticle reinforced lightweight metal composites	981
Self-assembly of NBR and NOMEX via electrospinning: rubbery NANOFIBERS for improving CFRP delamination resistance	986
Chemical compatibilizers as an approach to improve the mechanical properties of poly(propylene) reinforced with graphene nanoplatelets	994
Piezoresistivity of nanocomposites: accounting for CNT contact configuration changes	1002
Ionic polydimethylsiloxane-silica nanocomposites: from synthesis and characterization to self-healing property	1010
Mechanical behaviour of ultrathin carbon nanomembranes for water purification	1018
Intense pulsed light welding process with simultaneous mechanical roll-pressing for highly conductive silver nanowire/polyethylene terephthalate composites	1025
Surface functionalization of quartz fibres by direct growth of carbon nanostructures	1032
Characterisation of graphene-enhanced carbon-fibre/PEEK manufactured using spray-deposition and laser-assisted automated tape placement	1040
High speed imaging of the ultrasonic deagglomeration of nanoparticles in water	1048
Effects of microwave-assisted cross-linking on the creep resistance and measurement accuracy of the coaxial-structured fiber strain sensor	1056
Mechanics of reinforcement of polymer-based nanocomposites by 2D materials	1062
Enhanced mechanical properties of hierarchical MXENE/cf composites via low content electrophoretic deposition	1069
Remote field induced response of polymer nanocomposites embedded with surface-functionalised dielectric nanoparticles	1079
Effects of hybridization and ply thickness on carbon/carbon composite laminates strength and toughness	1091
Effect of weathering on the long-term performance of natural fiber reinforced recyclable polymer composites for structural applications	1097
Fibres hybridization for thermoplastic matrix composites	1104
Mechanical characterization of a three-dimensional hybrid woven composites	1112

Design and characterization of tough architected ceramic-based composites	1119
Bearing strength high performance fibre metal thin-ply laminates	1127
Visoelastic and VISCOPLASTIC creep modelling of short-glass fibre reinforced polypropylene composites	1130
3D printed short carbon fibres reinforced polyamide: tensile and compressive characterisation and multiscale failure analysis	1137
Estimation of interfacial shear strength of long glass fibre composites by x-ray computed tomography	1145
Material characterisation and fatigue data correlation of short fibre composites: effect of thickness, load ratio and fibre orientation at elevated temperature	1151
Local stress-strain behaviour in short glass fibre reinforced polymers - a comparison of different simulation approaches with experimental results based on x-ray computed tomography data	1159
Effect of fibre orientation, temperature, moisture content and strain rate on the tensile behaviour of short glass fibre-reinforced polyamide 6	1167
A mode II testing method for hybrid composites	1175
Deployable composite meshes – modelling, manufacture and characterisation	1183
Are pseudo-ductile all-carbon hybrid laminates notch insensitive in open hole tension?	1191
Reparability as a new function for high-performance pseudo-ductile hybrid composites	1197
On the optimal design of smart composite sensors for impact damage detection	1205
Impact properties of flax-carbon hybrid composites under low-velocity impact	1213
Enhancement of thin-ply composites translaminar toughness through fiber-hybridization: towards a discrimination with the ply thickness effect?	1220
Assessing the impact behavior of highly aligned fiber hybrid composites	1228
Development and characterization of hybrid thin-ply composite materials	1236
Tensile fatigue performance of carbon-carbon hybrid quasi-isotropic laminate	1244
Variable stiffness lattice structures	1251
Virtual-physical engineering of a graded CFRP/titanium aircraft suspension strut	1258
Manufacturing and properties of hybrid composites of continuous steel and glass fibers made by tailored fiber placement	1266
A novel hybrid thermoset-thermoplastic robot-based production concept for lightweight structural parts: a special view on the hybrid interface	1274
Tensile properties of deep drawn in-situ polymerized fiber-metal-laminates	1282
Micro-scale modelling of composites made of RCF/ PA6 staple fiber yarns with special emphasis on fiber length distribution	1290
Micro-ct based assessment of 3D braided AL2O3 reinforcement uniformity and permeability of all-oxide ceramic matrix composites production processes	1296
Multi-scale modeling of the thermo-viscoelastic behavior of 3D woven composites	1303

Advanced natural fibre textiles for composite reinforcement	1311
Characterization of interlock 3D permeability tensor for c-RTM process	1318
Automated g-code to FE mesh conversion - modelling polymer penetration into a textile to generate a polymer-textile composite made by additive manufacturing	1326
Micro-ct-based numerical validation of the local permeability map for the b-pillar infusion simulation	1333
Effect of temperature on damage onset in three-dimensional (3D) woven organic matrix composites for aero-engines applications	1341
Simulation of frictional contact interactions within jacquard harness of weaving looms for 3D interlock fabrics	1349
Laccase-enzyme treatment of flax fibres for improved interfacial strength in natural fibre composites	1357
DIC-based monitoring on DEBONDING crack propagation in wrapped composite joints	1362
Ultrasoft and hyperelastic electrically conductive nanocomposites for strain sensing applications . .	1369
Mechanical, rheological and thermal evaluation of poly(lactic acid) (PLA) / micro fibrillated cellulose (MFC) plasticized biocomposites produced with flat die extrusion and calendering	1377
Optimization of an exoskeleton	1384
Banana fibre as sustainable and renewable resource for reinforcement of polylactic acid	1391
Hybrid ratio effect on flexural properties for CFRP-natural fiber composite hybrid materials	1398
Investigation of energy absorption capacity of novel 3D-printed glass fibre reinforced thermoplastic bio-inspired structures	1404
Rapid fatigue life prediction of CFRP laminates by combining the data of self-heating with stiffness degradation	1412
Performance evaluation of e-skin for structural deformation detection	1420
Temperature detectable surface coating and self-sensing system with carbon nano-tube/epoxy composites	1426
Solubility behavior of graphene-oxide with various solvents	1433
Biodegradable polymer-based composites filled with biochar for tunable release of carvacrol	1437
Designing bicontinuous silica-epoxy nanocomposites	1445
Robust continuous production of carbon nanotube-grafted structural fibres: a route to hierarchical fibre reinforced composites	1451
Printed circuit boards made from cellulose fibrils	1457
Sandwich type shape memory polymer composite actuators to increase the recovery moment and deformability	1465
Supercritical CO ₂ assisted foam extrusion for aeronautical sandwich structure manufacturing	1472
Kinetic studies and its influence on phase transition behaviour of multicomponent amine-cured epoxy blend	1480

Non-isocyanate polyurethanes based composites: a new route to sustainable fully biobased structural composites	1486
MXENE nanoparticles to impart multifunctional properties to fibre reinforced plastic composites	1495
COMBOO – properties of a novel bamboo based honeycomb core material for composite sandwich structures	1500
Effect of aspect ratio and bulk density of carbon nanotube on the electrical conductivity of polycarbonate/multi-walled carbon nanotube nanocomposites	1508
Hierarchical solutions to compressive problems in fibre-reinforced composites	1512
Tough poly(ethylene glycol)-sized bacterial cellulose sheet for high impact strength laminated acrylic composites	1518
Experimental investigation and modelling of the morphology and induced thermal properties evolution by consolidation of flax fibres hybrid reinforced thermoplastic composite	1526
Avoiding complete failure of composite t-joints by embedding sacrificial cracks inside the BONDLINE	1536
Mechanical analysis of the indentation behavior of short fiber-reinforced composites using finite element method	1542
Micro-scale measurements on epoxy using in-situ microscopic techniques	1549
Study on cure-dependent properties of epoxy molding compound and warpage of semiconductor packages	1557
Thermoplastic coating on carbon fiber for the design of sustainable composite materials	1565
Fabrication of CNT aerogel composite through reactive infiltration of polyamide 6	1571
Void reduction in graphene interlayer enhanced carbon fibre thermoplastic composites	1579
Highly deformable and processable poly(3-hydroxybutyrate) in presence of FERULIC acid-based additives	1587
Chitosan nanoparticles with ginkgo BILOBA extract in an alginate carrier as a system for the slow release of the active substance	1595

A NOVEL BIO-INSPIRED MICROSTRUCTURE FOR PROGRESSIVE COMPRESSIVE FAILURE IN MULTIDIRECTIONAL COMPOSITE LAMINATES

Torquato, Garulli^a, Emile S., Greenhalgh^a, Silvestre T., Pinho^a

a: Faculty of Engineering, Imperial College London, UK – t.garulli@imperial.ac.uk

Abstract: *In this study we take inspiration from biological materials to design a modified microstructure for laminated multidirectional (MD) carbon fiber reinforced polymers (CFRP), with the objective of mitigating their compressive failure behavior. We introduce soft inclusions in the form of thin longitudinal strips of foam in 0° load bearing layers, aiming at arresting kinkband propagation. We conceived a bespoke stacking sequence and developed a tailored procedure for manufacturing the microstructure. We then performed in-situ tests on small scale notched specimens from a baseline laminate and a modified one. Results are presented and discussed.*

Keywords: Bioinspiration; Compression; Damage diffusion; Microstructural design

1. Introduction

Longitudinal compressive failure is a major concern for CFRP. In most high-performance unidirectional (UD) composites, failure occurs by fiber kinking. In regions of fiber misalignment, the matrix undergoes shear, leading to further fiber rotation. With increasing load, either this mechanism becomes unstable, or shear fracture of the matrix/interface occurs, leading to unstable collapse and to kinkband formation [1]. In MD laminates, the failure process is more complex and may involve delamination and some progressive damage in the off-axis plies [2]. However, almost inevitably, sudden compressive fracture of load bearing (0°) layers is the final event leading to catastrophic failure, with negligible detectable warning. These complexities lead to a lack of strategies to mitigate the failure process and improve performance.

In this work, we take inspiration from nature to design a novel microstructure for MD CFRP laminates. Several biological materials present alternating stiff and soft zones. The associated periodic stiffness variations are an effective strategy to enhance fracture resistance: a strong decrease in crack driving force occurs when the crack propagates from stiff to soft regions, eventually leading to crack arrest [3]. To replicate such a condition in a MD laminate undergoing compression, we modified its microstructure by replacing continuous 0° composite layers with alternating of stiff (0° composite) and soft (polymethacrylimide -PMI- foam) longitudinal strips, Figure 1, with the objective of creating regions where kinkbands may be arrested, favoring 0° composite strips to fail individually and independently, due to the soft strips isolating them.

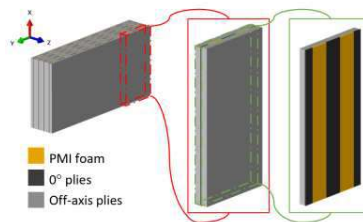


Figure 1. Simplified representation of the devised concept.

2. Material and methods

2.1 Materials

Since the soft inclusions are not load-bearing, a material with low specific weight is preferable for the soft inclusions. This, along with processing ease and compatibility, led to PMI foams being identified as optimal materials. PMI foam sheets, 0.07 mm thick, were provided by YoneshimaFelt Co. Ltd. Specifically, Rohacell® 200SL foam was used for this study (Table 1). The sheet thickness was chosen by considering commercial availability and compatibility in the design process.

Table 1: Rohacell® 200SL properties from [3].

Density [g/cm ³]	Tensile Modulus [MPa]	Compressive modulus [MPa]	Shear modulus [MPa]
0.205	371	370	123
	Tensile strength [MPa]	Compressive strength [MPa]	Shear strength [MPa]
	10.4	9.6	4.8

A 15gsm MR70/TP402 prepreg, commercially available from North Thin Ply Technologies (NTPT), was selected for this study. MR70 is a high-performance intermediate modulus carbon fiber; TP402 is a 135 °C curing epoxy used for automotive and aerospace applications. Properties for this material are not readily available from open literature, so, for the purpose of this study, they were estimated using micromechanics or assumed, as reported in Table 2 (with the standard notation used in [1]).

Table 2: MR70/TP402 properties.

Density [g/cm ³]	E ₁ [GPa] (compressive)	E ₂ [GPa]	G ₁₂ [GPa]	ν ₁₂
1.55	153.	9.5	3.16	0.26
X _t [MPa]	X _c [MPa]	Y _t [MPa]	Y _c [MPa]	S _L [MPa]
3880.	1800.	39.	160.	60.

2.2 Configuration design

To test the concept, we developed a bespoke stacking sequence to be used as a baseline, which we called Baseline-No-Foam (BNF), and a modified version for the new microstructure, named Foam Laminate (FL). The two laminate stacking sequences are as follows:

- BNF: $[\pm 45/(\pm 75/90/\pm 75/\pm 31_9/0)_{s_2}]_s$
- FL: $[\pm 45/(\pm 75/90/\pm 75/\pm 31_9/0_{2F})_{s_2}]_s$. Here the subscript F indicates the presence of the foam strips in the 0° layers

The BNF laminate was designed to have elastic properties similar to those of a commonly used industrial reference laminate (i.e. $[(\pm 45/0/\pm 45/90/0)_n]_s$) and to contain a reduced number of 0°

layers. Also, the high number of ± 31 layers was tailored to provide a strong support to the laminate at failure of the 0° layers. The FL sequence is obtained from the BNF one by doubling the number of 0° layers. In this case, however, 0° layers are intended as containing foam strips. Specifically, considerations of effectiveness and manufacturability led to the choice of having alternated 1 mm wide 0° composite and foam strips. Therefore, the BNF and FL laminates contain the same volume of composite material (and in the same orientations), the FL one being slightly thicker due to the presence of the foam.

2.3 Manufacturing

Prepreg sheets of the desired orientations were cut with a Blackman and White Genesis 2300 cutting machine. The BNF laminate was laid up manually according to standard practices. To prepare materials for the FL laminate, an Oxford Lasers Diode Pumped Solid State (DPSS) micro-machining system was used as follows:

- 0° prepreg layers, after being laid up in groups of four, $[0_4]$, were cut to have 1 mm wide rectangular slots in the fiber direction
- Foam sheets were cut, in their central region, to be divided into 1 mm wide strips
- PET sheets (125 μm thick) were cut to create templates for positioning of both the 0° prepreg layers and the foam strips

Lay-up of the foam laminate followed standard practices until each of the $[0_4]$ blocks, expected to contain foam strips, was reached; at this point a tailored procedure, exploiting the PET templates and involving multiple steps, was used to create the layer containing the foam strips. More in detail, the strips of 0° prepreg were laid first; afterwards, the foam strips were placed in the slots in between the prepreg. Figure 2 shows three stages of the process.

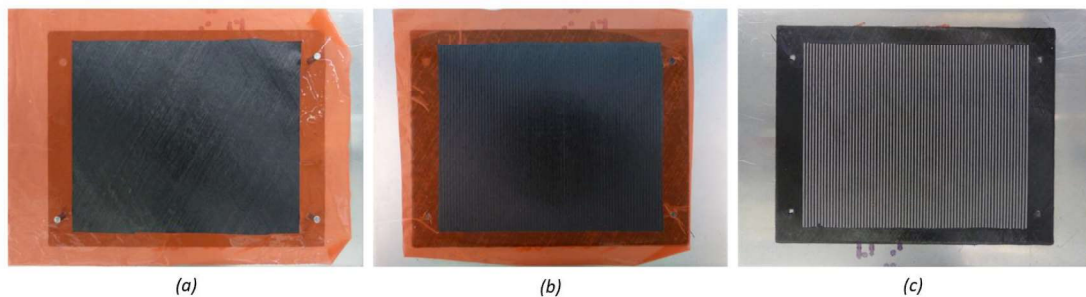


Figure 2. Three phases of the foam laminate lay-up procedure: (a) right before laying up a $[0_4]$ block containing the foam strips, (b) after laying up 0° prepreg strips, (c) after having laid up both prepreg and foam strips.

For this study, two small scale notched specimens for compression loading, Figure 3, were obtained from each of the two plates. The top and bottom faces of the specimens were ground parallel to ensure optimal loading during compression, while the notch was obtained by means of a disk saw; notch tip radius was found to be, by means of optical microscopy, consistently around 40-50 μm , figure 3 (c).

Due to an incident during manufacturing, the specimens' surface had to be slightly ground, which partially reduced their thickness (about 0.2 mm per specimen) and thus slightly modified their layup (by eliminating outer layers); this may have introduced some variability in the test

performed, but is not expected to have affected the qualitative observations presented here. Table 3 shows the ligament section dimensions and notch tip radii for the four specimens tested.

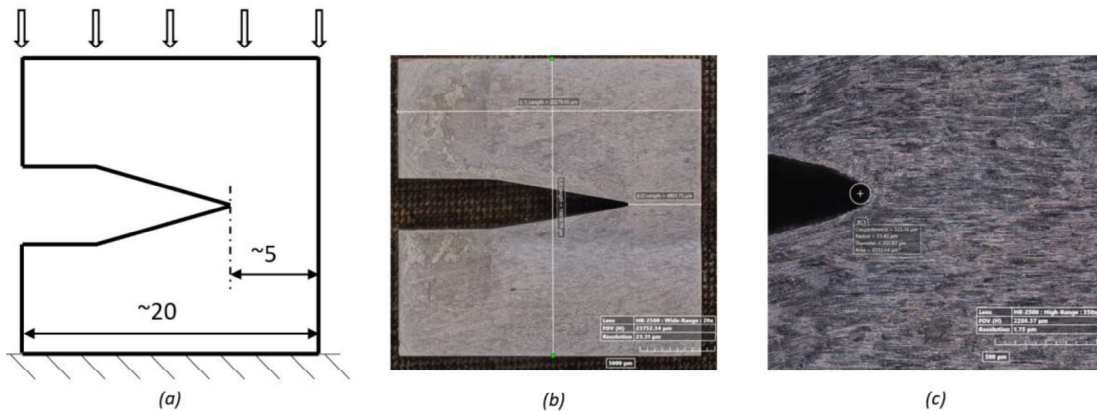


Figure 3. Small scale specimens manufactured: (a) nominal dimensions and loading scheme, (b) actual specimen microscopy with dimensions, (c) detail of the notch tip.

Table 3: Ligament dimensions and notch tip radii of the four specimens tested.

Specimen ID	Ligament length [mm]	Ligament thickness [mm]	Notch tip radius [μm]
BNF1	4.8	2.7	41
BNF2	4.8	2.7	51
FL1	4.9	2.9	43
FL2	4.8	2.9	48

2.4 Test method

The specimens were manually polished and gold coated. They were tested in compression, under displacement control, inside a Hitachi S-3700N SEM by means of a 5 kN in-situ loading stage from Deben UK. The displacement rate was set at 0.1 mm/min and data relative to jaws displacement and load were acquired at 10 Hz. The test was stopped at 400 N intervals to take SEM images of the specimen at different magnifications. The test was run either until complete failure of the specimen or up to a load of about 4.5 kN, in which case it was stopped to prevent damage to the load cell.

3. Results and discussion

The load-displacement curves for the specimens tested are reported in Figure 4. In these curves, small load drops correspond to relaxation occurring during the time the tests are stopped to take images. Both specimens containing foam strips, FL1 and FL2, did not fail by the end of the test. On the other hand, out of the two baseline specimens, BNF1 failed completely at a final load of about 3.83 kN, while specimen BNF2 did not fail by the end of the test.

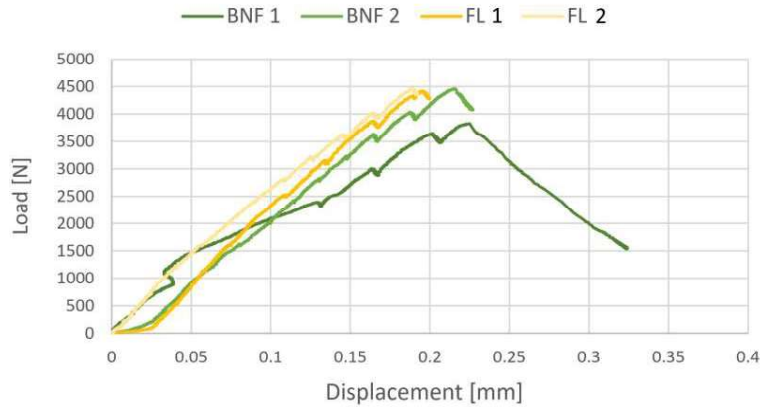


Figure 4. Load displacement curves for the four specimens tested.

Figure 5 shows SEM pictures of all specimens immediately before testing (Figure 5 (a)) and immediately after end of the tests (Figure 5 (b)). For all specimens, surface plies tended to delaminate from the rest of the specimen, and damage in the form of ply splits and fiber fracture is evident on them. By the end of the tests, for specimens BNF1 and BNF2, this damage extends from the notch tip all the way to the opposite specimen’s side, and the superficial plies are completely delaminated in this region. In FL1 and FL2 specimens, the damage observed on surface plies is less extended: for FL1, it extends to about 2 mm away from the notch tip; for specimen FL2 a little amount of damage is observed extending from the notch tip toward the bottom side of the specimen.

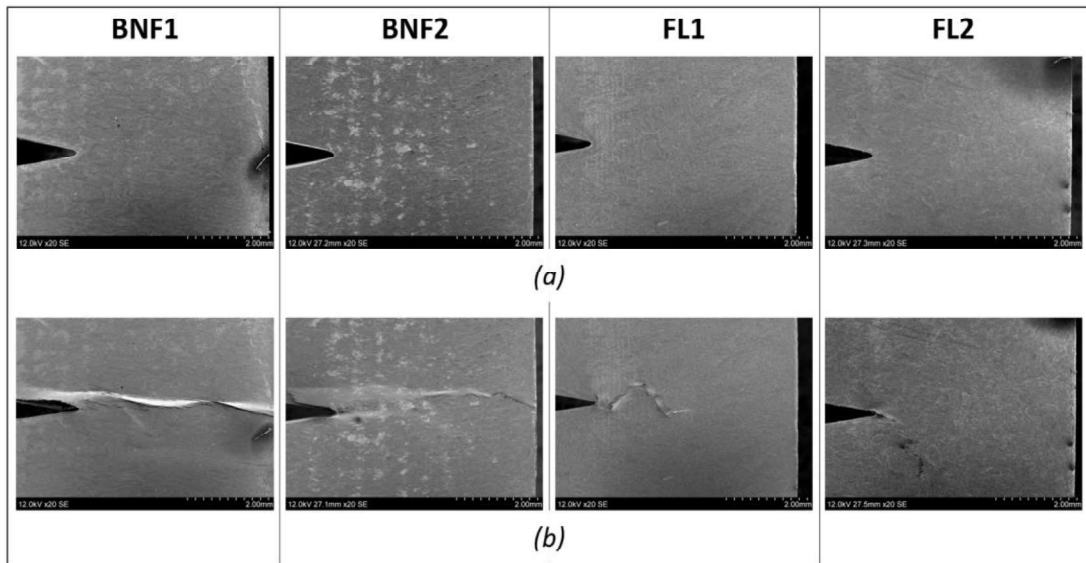


Figure 5. SEM pictures of the specimens’ ligament (a) before testing and (b) right after the test.

Figure 6 shows X-ray images of the specimens after testing. One feature common to all the specimens is the presence of clear fracture lines emanating from the notch tip, at an angle of $\pm 31^\circ$. The clarity with which these features are observed suggests that they might be somewhat continuous through the specimen thickness, for several layers. Considering the stacking sequence of the laminate (having $\pm 31^\circ$ ply blocks), it is hypothesized that these may have formed

by initial splitting of the layer with fiber orientation parallel to the direction of the fracture line and subsequent translaminar fracture of the layers with the opposite orientation. It is worth mentioning that X-ray images of FL1 and FL2 specimens show the striped pattern caused by the presence of the foam strips; these latter appearing darker in the images. From this it can be observed that, for both FL specimens, the tip of the notch is located in the middle of a dark region, that is in a region with foam strips.

Specimen BNF1, the only one that failed completely, shows a vast amount of damage going all the way from the notch tip to the opposite specimen's side. Damage probably consists mostly of kinkbands in 0° layers and translaminar fractures in $\pm 31^\circ$ layers. Additional splits at $\pm 31^\circ$ are also visible, as well as a wide delamination, as already seen from SEM observations. In specimen BNF2, a narrow damage band extends from the notch across almost the entire ligament length, accompanied by several splits, especially in the lower part of the specimen. Comparing this with BNF1, and considering that by the end of the test specimen BNF2 was still carrying a significant load, may suggest that the damage observed is limited to a few plies through the thickness, while most of the $\pm 31^\circ$ layers may still be intact and able to carry load. Delamination is also visible in the image, in an area enclosing all other damage observed. Specimen FL1 shows a similarly narrow band of damage extending for about 2.5 mm from the notch tip. An initial wider and brighter band cross a region without foam (lighter colored in the image); possibly this includes kinkbands in 0° layers and additional damage in other layers. As this band reaches the next region with foam strips (darker in the image), it divides into a 31° split, which then deviates into a -75° split, and an almost horizontal narrower band. These two narrow bands then reach the beginning of the next region without foam, where they arrest. Interestingly, specimen FL2 shows no damage at all, except for the already mentioned fracture lines originating from the notch tip. It is likely that these fracture lines and the foam strips present at the notch tip have acted as strong blunting factors, preventing significant stress concentration and damage initiation and propagation from the notch altogether.

Additional fractographic activities will help to fully understand the fracture behavior of the specimens.

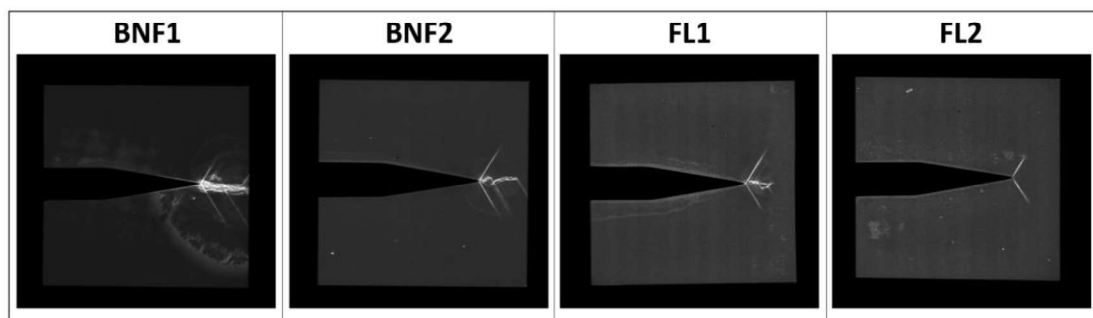


Figure 6. X-ray scans of the four tested specimens.

4. Conclusions

The study presented is concerned with the preliminary design, manufacturing and testing of a bioinspired microstructure for MD CFRP laminates aiming at mitigating compressive failure.

After designing a suitable configuration, a tailored procedure for manufacturing of the desired microstructure was developed. The procedure features adoption of laser cutting for the preparation of the composite prepreg and of the foam sheets used for creating the soft inclusions. Additionally, PET sheets are adopted to create templates for precise positioning of the two former components, with alignment being ensured by means of a system of alignment pins. The developed procedure allows precise manufacturing of the microstructure. In-situ tests were performed on four small scale notched specimens, two baseline ones and two containing soft inclusions. After the tests, X-ray imaging of the specimens was performed to gain a deeper understanding of the specimens' behavior. Out of the four specimens tested, only one baseline specimen failed completely; other tests had to be stopped to avoid damage to the rig's load cell. Our results suggest that splitting and translaminal fracture in off-axis plies from the notch tip occurred and acted as a strong crack blunting mechanism, reducing the stress concentration and the propensity to fracture initiation and propagation from the notch. While the results shown have to be expanded on further experimental activities, it was observed that specimens containing the soft inclusions had a reduced amount of damage when compared to baseline.

Further activities are underway to gain a deeper understating of the results obtained and produce further results to assess the effectiveness of the microstructure designed.

Acknowledgements

The authors kindly acknowledge the funding for this research provided by UK Engineering and Physical Sciences Research Council (EPSRC) programme Grant EP/T011653/1, Next Generation Fibre-Reinforced Composites: a Full Scale Redesign for Compression in collaboration with University of Bristol.

YoneshimaFelt Co. Ltd. and the person of Tomoya Yoneshima are kindly acknowledged for providing PMI foam sheets used for this research.

5. References

1. Pinho ST, Iannucci L, Robinson P. Physically-based failure models and criteria for laminated fibre-reinforced composites with emphasis on fibre kinking: Part I: Development. *Composites Part A: Applied Science and Manufacturing* 2006; 37:63-73.
2. Tsampas SA, Greenhalgh ES, Ankersen J, Curtis PT, On compressive failure of multidirectional fibre-reinforced composites: A fractographic study. *Composites Part A: Applied Science and Manufacturing* 2012; 43:454-468.
3. Kolednik O, Predan J, Fischer FD, Fratzl P. Bioinspired Design Criteria for Damage-Resistant Materials with Periodically Varying Microstructure. *Advanced Functional Materials* 2011; 21:3634-3641.
4. Rohacell® SL datasheet, accessed on 19/04/2022. https://www.rohacell.com/product/peek-industrial/downloads/rohacell%20sl_2020_january.pdf